Impact of fMRI Acoustic Noise on the Functional Anatomy of Visual Mental Imagery

A. Mazard[1], B. Mazoyer[1], O. Etard[1], N. Tzourio-Mazoyer[1], S.M. Kosslyn[2], and E. Mellet[1]

Abstract

■ One drawback of functional magnetic resonance imaging (fMRI) is that the subject must endure intense noise during testing. We examined the possible role of such noise on the activation of early visual cortex during visual mental imagery. We postulated that noise may require subjects to work harder to pay attention to the task, which in turn could alter the activation pattern found in a silent environment. To test this hypothesis, we used positron emission tomography (PET) to monitor regional Cerebral Blood Flow (rCBF) of six subjects while they performed an imagery task either in a silent environment or in an ''fMRI-like'' noisy environment. Both noisy and silent imagery conditions, as compared to their respective baselines, resulted in activation of a bilateral fronto-parietal network (related to spatial processing), a bilateral inferior temporal area (related to shape processing), and deactivation of anterior calcarine cortex. Among the visual areas, rCBF increased in the most posterior part of the calcarine cortex, but at level just below the statistical threshold. However, blood flow values in the calcarine cortex during the silent imagery condition (but not the noisy imagery condition) were strongly negatively correlated with accuracy; the more challenging subjects found the task, the more strongly the calcarine cortex was activated. The subjects made more errors in the noisy condition than in the silent condition, and a direct comparison of the two conditions revealed that noise resulted in an increase in rCBF in the anterior cingulate cortex (involved in performance monitoring) and in the Wernicke's area (required to encode the verbal cues used in the task). These results thus demonstrate a nonadditive effect of fMRI gradient noise, resulting in a slight but significant effect on both performance and the neural activation pattern. ■

INTRODUCTION

Over the course of the last 5 years, functional magnetic resonance imaging (fMRI) has supplanted positron emission tomography (PET) as the method of choice for neuroimaging studies. Researchers have come to appreciate that fMRI has superior sensitivity and spatial and temporal resolution. However, the acquisition of functional images using fMRI with EPI-BOLD sequences results in very intense noise, ranging from 100 to 114 dB (time average level), depending on the static magnetic field strength of the imager (Ravicz, Melcher, & Kiang, 2000). This noise is inherent in the gradient pulsing that is part and parcel of the fMRI acquisition process, and not only can make subjects uncomfortable but can also distract them from the cognitive task of interest. One may argue that the noise is present in all the conditions and thus will not affect the detection of activation. However, the effects of such noise may not be strictly additive: If the cognitive task requires effort, noise may have a larger effect on processing than during the standard ''off'' condition used as a baseline.

For example, fMRI noise can impair the auditory cortex's ability to process auditory stimuli (Elliott, Bowtell, & Morris, 1999; Talavage, Edmister, Ledden, & Weisskoff, 1999; Talavage, Ledden, Benson, Rosen, & Melcher, 2000; Bandettini, Jesmanowicz, Van Kylen, Birn, & Hyde, 1998; Ulmer, Biswal, Mark, et al., 1998; Ulmer, Biswal, Yetkin, et al., 1998). This effect has been interpreted as reflecting the saturation of the auditory cortex during baseline conditions, which in turn reduces the dynamic range of the response during the test conditions. Other studies have assessed the effect of noise on activation arising during visual and motor tasks (Elliott et al., 1999; Bandettini et al., 1998; Cho, Chung, Lim, & Wong, 1998). Some of these studies found an increase of motor activation and a decrease of visual activation (Cho et al., 1998) whereas others reported no effect (Elliott et al., 1999; Bandettini et al., 1998). Note that these latter studies used very simple tasks and with minimal cognitive demands (such as finger tapping and perception of a reversing checkerboard). During a complex task, the noise could disrupt the subject's attention, and thus impair performance. Since it has been shown that both the level of performance and the amount of effort paid to the task may affect the pattern of activation

[1]CNRS UMR 6905, CEA, Université de Caen and Paris V, [2]Harvard University

(Kiehl, Liddle, & Hopfinger, 2000; Carter et al., 1998; Tagaris et al., 1997), fMRI noise during a complex cognitive task may in turn alter the activation pattern. In this case, some of the apparent activation detected using fMRI could be induced by the noise rather than reflecting the processing of the task itself. For example, in the visual domain, the brain areas responsive to attentional load and task difficulty might be more active when a complex task is performed in noise than in silence. In particular, one may expect that frontal and parietal regions, shown to play a key role in top-down control (Kanwisher & Wojciulik, 2000; Kastner & Ungerleider, 2000; Coull, 1998), and the anterior cingulate cortex, involved in performance monitoring (MacDonald, Cohen, Stenger, & Carter, 2000), would be more active in noisy than silent conditions.

In addition, noise could affect early visual areas (i.e., Brodmann's areas 17 and 18), the activity of which increases when attention in the relevant modality is stronger (Kanwisher & Wojciulik, 2000; Kastner & Ungerleider, 2000). Moreover, the intense auditory noise produced during fMRI may produce cross-modal inhibition of visual cortex (Woodruff et al., 1996), especially in a low-level baseline condition during which the subject's attention is not mobilized by the task and may thus be distracted by noise. The combination of these two factors—an increase during a cognitive task and a decrease during a baseline task—may bias the detection of activation in early visual areas.

The possible effects of noise on early visual cortex is of particular interest regarding a current controversy in the study of visual mental imagery (Kosslyn & Ochsner, 1994; Roland & Gulyãs, 1994; see also Thompson & Kosslyn, 2000; Mellet, Petit, Mazoyer, Denis, & Tzourio, 1998). Some researchers have reported activation of early visual cortex whereas others have not, but the reasons for this disparity are not clear. For example, some researchers suggested that retinotopically organized visual cortex is involved only when a high spatial resolution mental image is created (Thompson & Kosslyn, 2000; Kosslyn, Thompson, & Alpert, 1997). However, recent studies have challenged this hypothesis by demonstrating that early visual cortex is if anything deactivated during a visual imagery task that required high spatial resolution (Mellet, Tzourio-Mazoyer, et al., 2000) or is activated to equal extents when subjects visualize high and low spatial frequency gratings (Thompson, Kosslyn, Sukel, & Alpert, 2001).

In the present study, we tested the hypothesis that "fMRI-like" noise could affect the detection of activation in early visual cortex, and more generally we assessed the effect on both behavior and neural activation of "fMRI-like" noise during a mental imagery task. Previous studies that focused on the effect of fMRI noise had to resort to tricks to reduce noise during the baseline condition (e.g., earplugs or sparse methods using fast acquisition). In the present study, we used PET—which is inherently silent—and introduced noise by playing back previously recorded fMRI noise of a clinical EPI-BOLD sequence. We chose an imagery task that requires high spatial resolution that has previously been shown to produce decreased activity in calcarine cortex, when performed in a silent environment (Mellet, Tzourio-Mazoyer et al., 2000). The subjects were asked to judge subtle aspects of prelearned 3-D geometric scenes (Figure 1 provides an illustration of one of the scenes). They visualized one scene, then they heard the labels of two positions on the base and a statement of relative height; they were to consult their image and decide whether statement correctly characterized the relative heights of the scene above the two named positions on the base. In addition to the imagery condition, subjects simply heard the stimuli and responded without visualizing or making judgments; this was the baseline condition. A rest control condition was also included, and consisted of lying silently with eyes closed, as in all conditions, with no particular instruction except to refrain from moving. In addition, we recorded the number and amplitude of horizontal eye movements during the tasks. These behavioral data may act as an index of the scanning of mental images (Pollen & Trachtenberg, 1972).

In order to assess the effects of noise, each condition was performed twice by the same subjects, either in a truly silent or in the "fMRI-like" sound environment. Using ^{15}O-labeled water, 12 sequential PET measure-

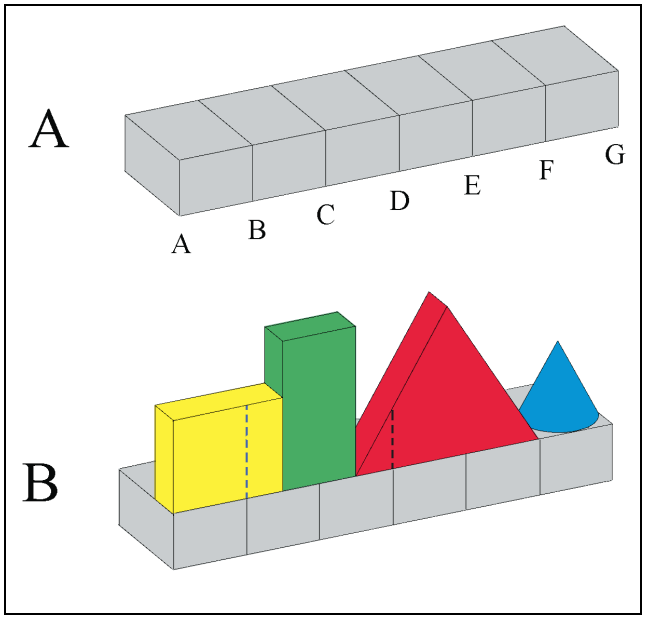

Figure 1. (A) The base on which four geometric shapes were placed. Before the PET experiment, each subject learned the locations specified by the letters. (B) An example of a typical 3-D scene that the subject had to learn from a visual presentation. During the PET measurements, subjects, eyes closed, had to form a visual mental image of the scene and evaluate statements about height comparisons, such as "B higher than D," heard through earphones. In the present example, the answer would be "true."

Table 1. Comparison Analysis Revealing Foci of Significant NrCBF Increases Between Imagery Versus Baseline and $Imagery_{No}$ Versus $Baseline_{No}$

	Coordinates							
	Imagery Versus Baseline				*$Imagery_{No}$ Versus $Baseline_{No}$*			
Anatomical Location of Maximum Voxel	*x*	*y*	*z*	*Z Score*		*y*	*z*	*Z Score*
L. precuneus/parieto-occipital sulcus					−6	−72	48	4.4
	−16	−70	48	5.6	−30	−60	48	5.6
L. inferior parietal gyrus	−46	−42	48	3.8				
R. precuneus/parieto-occipital sulcus	18	−70	50	5.3	42	−76	30	4.4
R. superior parietal gyrus	28	−68	60	5.1				
L. superior frontal sulcus	−26	6	58	4.2	−24	6	54	5.5
L. precentral gyrus					−36	−6	46	4.3
L. precentral sulcus	−54	8	32	3.2	−46	4	26	3.4
R. superior frontal sulcus	32	0	50	4.6	32	2	48	3.5
R. middle frontal gyrus					44	−4	52	3.3
					40	10	54	3.2
L. inferior frontal sulcus/precentral sulcus	−48	28	30	3.6	−42	20	30	3.8
R. inferior frontal sulcus	50	30	22	3.5	48	30	26	3.6
L. superior frontal sulcus (ant. part)	−26	58	12	3.5				
	−24	70	10	3.6				
R. anterior cingulate cortex					8	30	22	4.4
R. anterior/median cingulate cortex					8	16	30	4.5
R. median frontal gyrus					4	10	50	3.9
L. anterior insula					−32	22	−2	3.8
R. anterior insula					40	20	−6	3.5
R. middle temporal/middle occipital gyrus	60	−50	−14	4.3	74	−46	−6	3.9
					68	−26	−12	3.3
L. inferior temporal gyrus (post. part)	−48	−66	−6	3.7	−50	−60	−8	3.1
	−52	−50	−12	3.2				
Cerebellar vermis	2	−62	−12	4.6	6	−54	−22	3.9
	0	−70	−38	3.8	4	−66	−32	4.0
	4	−46	−20	3.7	10	−76	−26	3.8
L. cerebellar cortex	−28	−68	−36	4.5	−26	−68	−32	3.5
	−32	−54	−30	3.7	−6	−80	−30	3.1
R. cerebellar cortex	30	−56	−36	3.7				
	14	−44	−46	3.9				
R. thalamus					4	−22	−2	3.4
	8	−10	6	3.4				
L. thalamus					−2	−2	0	3.1
Pons					2	−22	−40	3.2

The data, based on six subjects, are local maxima detected with SPM 99 software. Activated region volumes are given in voxels. Within these regions, the anatomical localization of the maximum *Z* scores of the voxel is given on the basis of the MNI template, using their stereotactic coordinates in mm (R.=right; L.=left).

ments of regional cerebral blood flow (rCBF) were obtained for six conditions: those performed in silence will be referred to as "silent imagery" (imagery), "silent baseline" (baseline), and "silent rest" (rest); those performed in noise will be referred to as "imagery–noise" ($imagery_{No}$), "baseline–noise" ($baseline_{No}$), and "rest–noise" ($rest_{No}$).

RESULTS

Behavioral Results

Responses and Response Times

During PET measurements, we recorded the number of correct responses as well as the response times. In mental imagery conditions, the subjects clearly performed better than chance (50%) in both noisy and silent environments [$p = .001$ for imagery, 89.9 ± 11.6%, and $p = .01$ for $imagery_{No}$, 74.2 ± 18.2%, $\chi^2(10)$]. These behavioral data are very close to those reported in a previous study using the same task design (Mellet, Tzourio-Mazoyer et al., 2000). However, all subjects but one reported that they had much more difficulty forming a clear and vivid image in the noisy environment than in silence. Consistent with these reports, the number of correct responses was lower in the presence of noise than in silence [$t(10) = 2.4$, $p = .03$, paired t test], showing that noise did indeed disrupt performance.

The response times were not significantly different between the two imagery conditions [9.256 ± 3.72 sec during imagery and 9.106 ± 3.98 sec during $imagery_{No}$; $t(10) = .09$, $p = .92$, paired t test]. In addition, we did not find a correlation between response times and number of correct responses [$r(21) = -.15$, $p = .50$], which belies a possible speed–accuracy tradeoff.

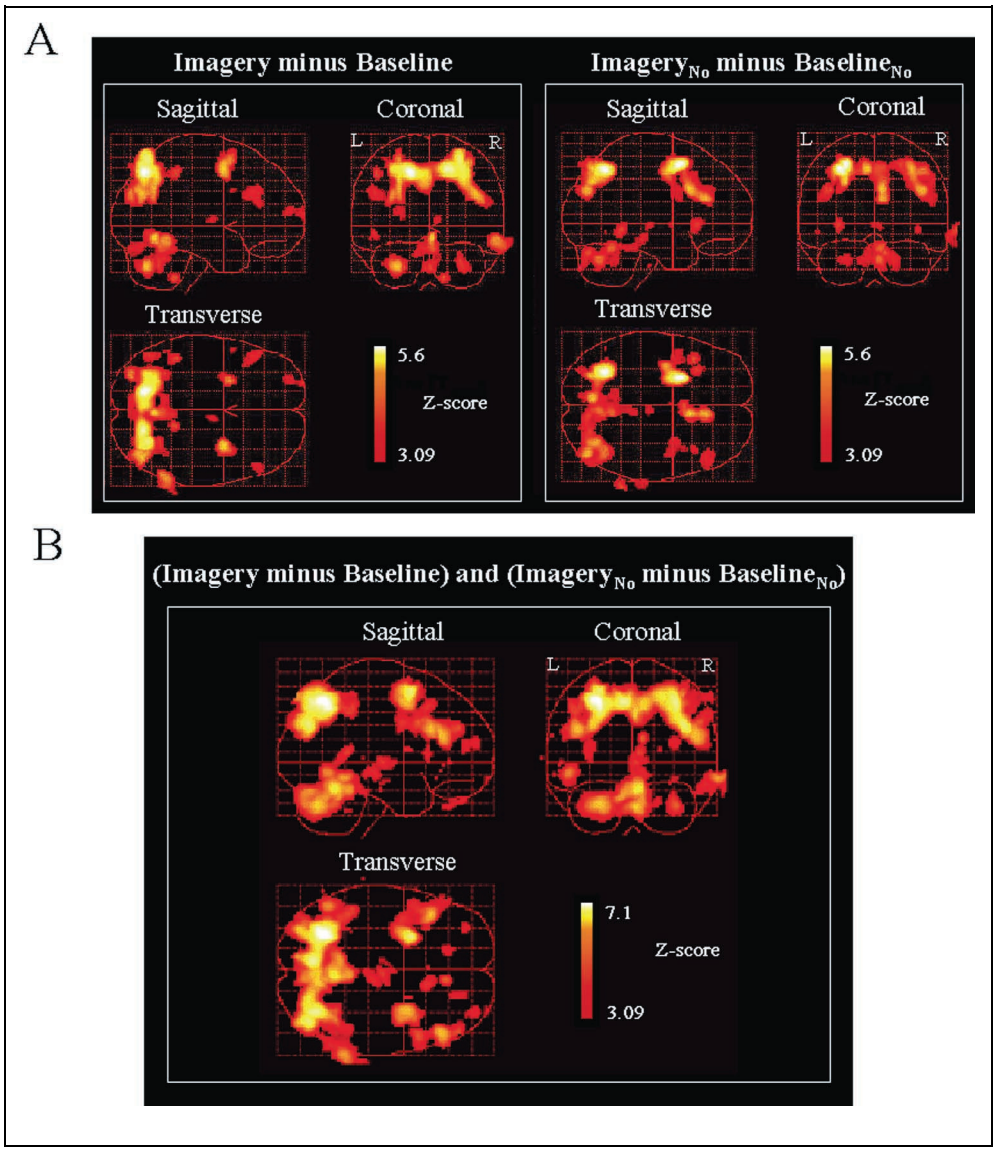

Figure 2. (A) Statistical parametric map revealing the areas that were activated when subjects formed images compared to baseline conditions in a silent environment (left) and "fMRI-like" noise (right). (B) Statistical parametric map revealing the common areas that were activated when subjects formed images compared to baseline conditions (conjunction analysis), whichever the sound environment. Volumes were thresholded to project in three orthogonal directions: sagittal, coronal, and transverse, and reach threshold at $Z = 3.09$ ($p < .001$, uncorrected for multiple comparison). Stereotactic coordinates of local maxima are given in Tables 1 and 2.

Eye Movements Analysis

Horizontal eye movements occurred equally frequently in all conditions [$F(5,3) = .57$, $p = .72$]. In contrast, the amplitude of eye movement was different across conditions [$F(5,3) = 3.80$, $p = .01$]. Post hoc analysis revealed that this difference was due to higher amplitude during the imagery tasks (mean = 6°) than during their respective baseline [mean = 5°, $t(5) = 2.66$, $p = .04$, paired t test] and rest conditions [mean=5°, $t(5) = 2.49$, $p = .05$, paired t test]. Note that the amplitude during the baseline conditions was no different from that during the rest conditions [$t(5) = .16$, $p = .87$, paired t test].

Finally, comparable numbers and amplitudes of eye movements occurred in the noise conditions ($imagery_{No}$, $baseline_{No}$, and $rest_{No}$) and in the corresponding silent conditions (imagery, baseline, and rest) [$t(5) = .55$, $p = .6$, paired t test]. Thus, any differences between the silent and noise conditions cannot be ascribed to differences in eye movements made during those conditions.

PET Results

We report specific comparisons designed to discover possible effects of noise on neural activation during imagery.

Table 2. Conjunction Analysis Revealing Foci of Significant NrCBF Increases Common to Imagery and $Imagery_{No}$ as Compared to Baseline and $Baseline_{No}$: ($Imagery_{No}$ vs. $Baseline_{No}$) and (Imagery vs. Baseline)

	Coordinates			
Anatomical Location of Maximum Voxel	*x*	*y*	*z*	*Z Score*
L. precuneus	−28	−64	50	7.1
L. precuneus/parieto-occipital sulcus	−6	−72	48	6.6
R. precuneus/superior occipital gyrus	34	−70	48	6.4
L. superior frontal sulcus	−26	6	58	6.3
L. inferior frontal sulcus	−44	22	28	5.2
L. inferior frontal/precentral sulcus	−40	0	32	4.1
R. superior frontal sulcus	32	2	48	5.3
R. inferior frontal sulcus	50	30	22	5.3
R. inferior frontal sulcus	54	12	32	4.4
R. inferior frontal sulcus/middle frontal gyrus	50	44	28	4.4
R. superior frontal sulcus (anterior part)	34	56	16	3.8
L. superior frontal sulcus (anterior part)	−32	50	12	3.7
R. anterior cingulate cortex	8	34	20	4.5
R. anterior/median cingulate cortex	14	18	44	4.1
L. anterior insula	−34	20	8	3.7
R. middle temporal/middle occipital gyrus	68	−48	−12	5.0
R. inferior occipital gyrus	60	−60	−18	3.9
R. inferior occipital gyrus	74	−34	−20	3.7
L. middle temporal/middle occipital gyrus	−50	−60	−8	4.8
Cerebellar vermis	4	−54	−22	5.7
Cerebellar vermis	4	−68	−36	5.4
L. cerebellar cortex	−26	−68	−32	5.3
R. cerebellar cortex	34	−54	−32	4.4
R. thalamus	4	−16	0	4.1
R. thalamus	8	−24	−8	4.0

Imagery Compared to Baseline and Imagery$_{No}$ Compared to Baseline$_{No}$ (Table 1 and Figure 2)

These analyses included two contrasts: imagery versus baseline and imagery$_{No}$ versus baseline$_{No}$. The set of activated regions revealed by these two contrasts was very close to that reported by Mellet, Tzourio-Mazoyer, et al. (2000). The two patterns of activation also shared a large set of activated regions. These regions will be discussed in the following section, on the conjunction analysis. First, we focused on one region of interest: calcarine cortex. These contrasts did not reveal any activation of the calcarine cortex either in silent or in ''fMRI-like'' noise conditions, at a .001 confidence level or at level below the statistical threshold (data not shown here).

Conjunction Between Noisy and Silent Imagery

This analysis revealed the activations and deactivations common to both noisy and silent imagery conditions.

CBF increases (Table 2 and Figure 2). We found activation in the parietal lobe, including the intraparietal sulcus and the precuneus and extending to the right superior occipital gyrus. In addition, we detected several foci in the frontal lobe, including bilateral activation in the depth of the superior frontal sulcus (which extended downwards in the left hemisphere), bilateral activation of the inferior frontal sulcus, and bilateral activation of the anterior part of the superior frontal sulcus.

We also detected two foci of activation in the right anterior part of the anterior cingulate cortex extending to the median part and bilateral activation at the junction of the posterior part of the middle temporal gyrus and the middle occipital gyrus. These last two regions are part of the so-called ventral pathway. Finally, the cerebellar vermis and bilateral cerebellar cortex were activated, as well as the ponto-mesencephalic tegmentum.

CBF decreases (Table 3). This conjunction included comparisons between baseline$_{No}$ versus imagery$_{No}$ and baseline versus imagery, revealing regions that were deactivated in both imagery tasks in either sound environment. The main finding was that visual areas were deactivated in regions very close to those found earlier by Mellet, Tzourio-Mazoyer et al. (2000). We found these deactivations ventrally in the bilateral collateral sulcus, extending to the left lingual gyrus and the bilateral calcarine sulcus, and dorsally in the bilateral cuneus, again extending to the calcarine sulcus. Finally, we found a distinct and more distant deactivation in the bilateral inferior occipital gyrus.

A complete list of other deactivated regions is provided in Table 3, which includes the most ventral part of the left anterior cingulate cortex and a more medial part of this cortex. In the frontal lobe, we found bilateral deactivation extending to the anterior part from a most dorsal part of the superior frontal gyrus. In addition, blood flow decreased bilaterally in the central sulcus, and also decreased bilaterally in the

Table 3. Conjunction Analysis Revealing Foci of Significant NrCBF Decreases Common to Imagery$_{No}$ and Imagery as Compared to Baseline$_{No}$ and Baseline, Respectively: (Baseline$_{No}$ vs. Imagery$_{No}$) and (Baseline vs. Imagery)

Anatomical Location of Maximum Voxel	*Coordinates*			*Z Score*
	x	*y*	*z*	
L. collateral sulcus	−22	−72	−10	5.5
L. calcarine sulcus	−28	−72	4	4.7
L. cuneus/calcarine sulcus	−16	−96	20	4.6
L. calcarine sulcus	−10	−92	16	4.6
L. intraoccipital sulcus	−14	−90	34	3.3
L. lingual gyrus	−4	−76	0	3.2
R. collateral sulcus	24	−72	−8	4.8
R. calcarine sulcus	26	−78	8	4.0
R. occipital transverse sulcus	34	−86	14	3.7
R. cuneus	12	−90	22	4.3
R. cuneus	22	−98	14	3.7
L. inferior occipital gyrus	−34	−90	−6	5.3
R. inferior occipital gyrus	44	−84	−14	3.9
L. ventral anterior cingulate cortex	−4	30	−14	4.8
Corpus callosum	−10	−10	32	5.0
L. anterior cingulate cortex	−10	−24	40	4.6
R. median frontal gyrus	16	−12	58	4.4
L. superior frontal gyrus	−8	56	30	5.4
L. superior frontal gyrus	−10	60	12	5.0
L. central sulcus (superior part)	−28	−30	64	5.3
R. central sulcus (superior part)	22	−46	60	5.2
R. central sulcus (superior part)	56	−16	24	5.0
R. posterior insula/supramarginal gyrus	46	−38	26	5.0
R. middle temporal gyrus	50	−2	−22	4.9
L. supramarginal gyrus	−62	−26	22	4.1
L. angular gyrus	−52	−68	34	3.8
L. precentral sulcus	−60	−6	24	5.1
L. hippocampus	−28	−10	−18	5.6
L. inferior temporal sulcus	−48	−10	−28	5.2
L. parahippocampal gyrus	−36	−8	−10	4.5

Table 4. Foci Where NrCBF Variations (ΔNrCBF) During $Imagery_{No}$ as Compared to $Baseline_{No}$ Were Significantly Larger Than ΔNrCBF During Imagery as Compared to Baseline: ($Imagery_{No}$–$Baseline_{No}$) Minus (Imagery–Baseline) Masked by ($Imagery_{No}$–$Baseline_{No}$)

Anatomical Location of Maximum Voxel	*Coordinates*			
	x	*y*	*z*	*Z Score*
L. posterior superior temporal sulcus	−48	−42	12	4.1
R. dorsal anterior cingulate cortex	8	14	28	3.8
R. dorsal anterior cingulate cortex	4	8	44	3.1
R. inferior frontal gyrus (pars orbitalis)	42	36	−18	3.4
R. pons	4	−22	−34	3.3
Calcarine sulcus (posterior part)	0	−102	−2	2.9*

*$p < .005$.

supramarginal and postcentral gyrus, extending to the precentral gyrus on the left hemisphere. In both hemispheres, this cluster spread to the middle temporal gyrus and to the hippocampus on the left side.

Effects of Noise

The results of greatest interest focus on the effects of noise per se, which are revealed by the following comparisons: a comparison of $imagery_{No}$ versus $baseline_{No}$ and imagery versus baseline activation maps were computed in order to highlight activations that were specific or higher in the $imagery_{No}$ task as compared to the imagery task; and the three conditions performed in the presence of noise ($rest_{No}$, $baseline_{No}$, and $imagery_{No}$) were compared with the three corresponding conditions performed in silence (rest, baseline, and imagery).

Effects of noise on the activation pattern during the mental imagery task (Table 4). These activations reflected the interaction between the imagery tasks and the gradient pulsing noise, as revealed by the following comparison: ($imagery_{No}$ – $baseline_{No}$) minus (imagery–baseline) masked by the $imagery_{No}$ – $baseline_{No}$ contrast (see Methods). We compared the two imagery conditions to discover which areas were more active when images were generated in an "fMRI-like" sound environment. Only four foci of activation reached the .001 level of significance. We found effects of noise in the posterior superior temporal sulcus, a region included in Wer-

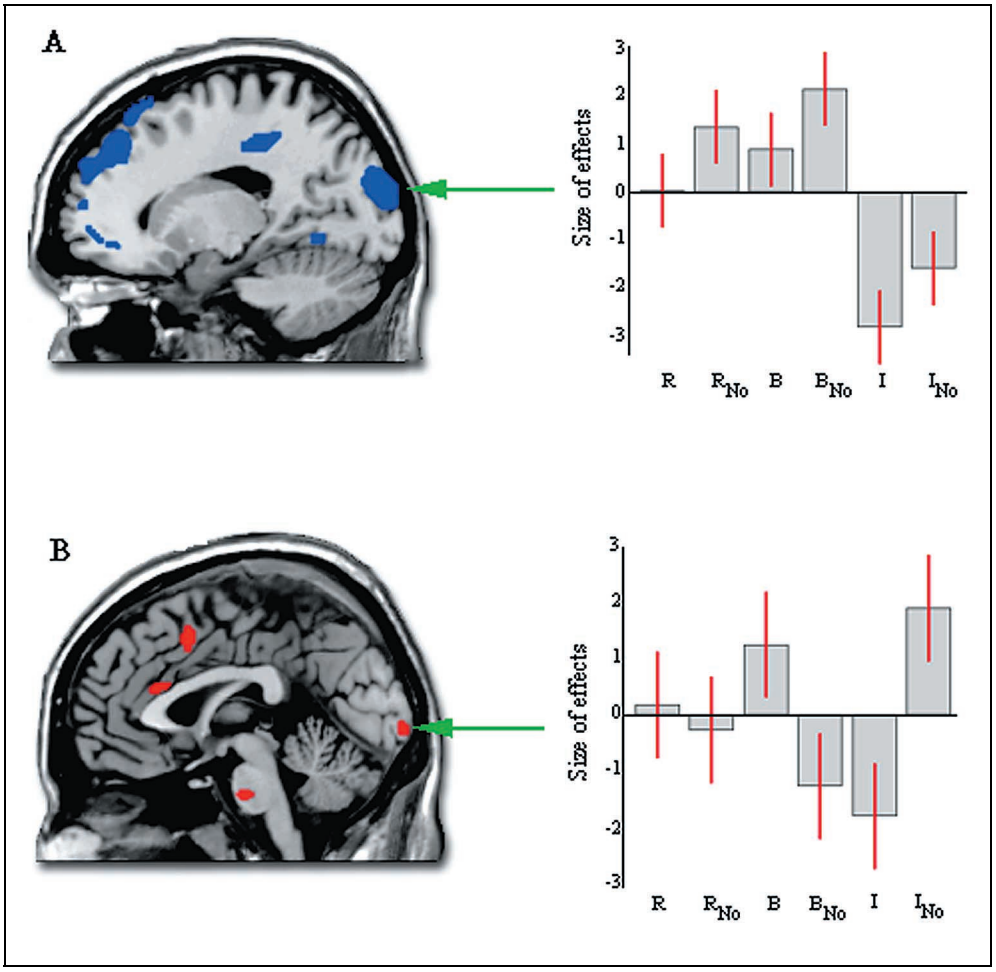

Figure 3. (A) Deactivation in medial occipital cortex (cuneus: $x = -16, y = -96, z = 20$) during both mental imagery tasks and histogram of the size of effects of interest of this focus (R = rest; R_{No} = $rest_{No}$; B = baseline; B_{No} = $baseline_{No}$; I = imagery; I_{No} = $imagery_{No}$). Stereotactic coordinates of local maxima are given in Table 3 ($p < .001$, uncorrected for multiple comparison). (B) Activation in the posterior part of the calcarine cortex ($x = 0$, $y = -102, z = -2$) during the $imagery_{No}$ ($p < .005$, uncorrected for multiple comparison).

nicke's area. In the frontal lobe, the largest activation was located in the right anterior part of the cingulate cortex, and we found activation in the pars orbitalis of the right inferior frontal gyrus. Finally, we detected activation in the pons.

Given the controversy about the role of the calcarine cortex in visual mental imagery (e.g., Thompson & Kosslyn, 2000; Mellet et al., 1998), we were particularly interested in the effect of noise on this area. Thus, we examined the activation maps at a more permissive significance level ($p < .005$, uncorrected for multiple comparisons). At this threshold, we found activation within the most posterior part of the calcarine cortex ($p = .002$). As shown in Figure 3, this activation was negative in imagery and positive in baseline whereas it was positive in $\text{imagery}_{\text{No}}$, and negative in $\text{baseline}_{\text{No}}$.

Correlation analyses between accuracy, response times, and calcarine cortex activation. We asked whether the amount of activation in the calcarine cortex correlated with accuracy and with response times. Linear regressions were computed between the normalized rCBF (NrCBF) of the maximal activated calcarine cluster and the accuracy (number of correct responses), and between NrCBF and response times recorded for each subject in each imagery condition. The analyses were performed for both mental imagery conditions combined as well as separately for imagery and $\text{imagery}_{\text{No}}$ conditions. First, we did not find any correlation between accuracy and the blood flow values in the calcarine cortex when we combined data from both mental imagery conditions [$r(21) = -.16$, $p = .61$]. However, when we computed separate correlations for the two conditions, we found that the blood flow values in the calcarine cortex during the imagery condition were significantly negatively correlated with accuracy [$r(10) = -.95$, $p = .004$]. In contrast, we did not find a correlation between accuracy and blood flow in the $\text{imagery}_{\text{No}}$ condition [$r(10) = -.15$, $p = .77$].

In addition, we did not find a correlation between response times and the blood flow values in the calcarine cortex when data were combined from both imagery conditions [$r(21) = -.41$, $p = .18$]; moreover, we failed to find such a correlation even when we computed separate analyses for imagery and $\text{imagery}_{\text{No}}$ conditions [$r(10) = -.41$, $p = .42$ and $r(10) = -.51$, $p = .30$, respectively].

Effect of noise in each condition.

REST_{NO} VERSUS REST (TABLE 5, TOP). This contrast revealed bilateral activation within the temporal lobe, including the Heschl's gyrus and the planum temporale.

$\text{BASELINE}_{\text{NO}}$ VERSUS BASELINE (TABLE 5, MIDDLE). In this comparison, the most significant activation was localized in the posterior part of the right cerebellar hemisphere. In the occipital lobe, we found activation in two portions of the left middle occipital gyrus, with one in the more medial part of this gyrus. In the frontal lobe, we found activation in the right middle frontal gyrus together with the left precentral gyrus and the left rolandic operculum. A cluster localized in the left anterior cingulate cortex was also activated. Note, however, that we neither detected activation in the primary nor in secondary auditory cortex.

$\text{IMAGERY}_{\text{NO}}$ VERSUS IMAGERY (TABLE 5, BOTTOM). This contrast revealed activation in the right superior frontal gyrus, in the adjacent anterior cingulum, and in the left inferior frontal gyrus together with the adjacent anterior insula. In the temporal lobe, the left Heschl's gyrus, the superior temporal gyrus bilaterally, and the left temporal pole were activated. The paracentral lobule was also activated.

Again, we focused on the effect of noise in the calcarine cortex during visual mental imagery, and examined the activation map at a $p < .005$ level of significance. At this threshold, we found activation within the most posterior part of the calcarine cortex ($p = .004$).

To sum up the PET results, the comparison between imagery and baseline revealed only a deactivation of the medial part of the calcarine cortex ($p = .001$). Similarly, we observed such deactivation in the comparison between $\text{imagery}_{\text{No}}$ and $\text{baseline}_{\text{No}}$ ($p = .001$). In sharp contrast, we found an activation of the posterior part of the calcarine cortex during the $\text{imagery}_{\text{No}}$ condition, but only when compared to imagery and when we contrasted imagery versus baseline ($p < .005$).

DISCUSSION

The purpose of the present study was to assess the effect of fMRI scanner noise on performance and the pattern of neural activation during an effortful mental imagery task. We will focus on two sets of results. The first reflects the difference between the contrasts ($\text{imagery}_{\text{No}}$ vs. $\text{baseline}_{\text{No}}$) minus (imagery vs. baseline). This contrast highlighted the effect of noise on the activation pattern during imagery. Any activation revealed by this contrast shows that fMRI gradient noise, although constant across conditions, does not result in a purely additive effect. The second type of contrast compares each noise condition with the corresponding silent condition, which provides a direct measure of the effects of noise, particularly in the auditory cortex.

Areas Activated by Both Mental Imagery Tasks (Figure 2)

We first return to the activation pattern elicited in common by the two imagery conditions, as revealed by the conjunction analysis. Although the subjects re-

Table 5. Foci of Activations During the Noise Conditions ($Imagery_{No}$, $Baseline_{No}$, and $Rest_{No}$) as Compared to Silent Conditions (Imagery, Baseline, and Rest)

Anatomical Location of Maximum Voxel	*Coordinates*			
	x	*y*	*z*	*Z* score
$Rest_{No}$–Rest				
R. superior temporal/Heschl's gyrus	50	−26	6	4.5
L. Heschl's gyrus	−40	−24	8	4.0
L. superior temporal gyrus	−60	−26	6	3.2
$Baseline_{No}$–Baseline				
R. cerebellar hemisphere (crus I)	6	−88	−24	3.9
L. middle occipital gyrus	−32	−88	8	3.6
L. middle occipital gyrus (medial part)	−26	−64	18	3.3
R. middle frontal gyrus	32	36	8	3.6
L. precentral sulcus	−66	−10	34	3.5
L. rolandic operculum	−38	−10	26	3.8
L. ventral anterior cingulate cortex	−14	38	−6	3.4
$Imagery_{No}$–Imagery				
R. superior frontal gyrus/dorsal anterior cingulate cortex	14	46	44	3.9
R. anterior superior frontal gyrus	12	64	4	3.6
L. inferior frontal gyrus/anterior insula	−34	30	2	3.3
L. Heschl's gyrus	−36	−24	8	3.9
L. superior temporal sulcus (posterior part)	−46	−40	12	3.3
R. superior temporal gyrus	38	−36	12	3.3
L. superior temporal sulcus	−58	−16	−4	3.6
L. inferior temporal gyrus/temporal pole	−40	−2	−38	3.3
Paracentral lobule	−14	−38	54	3.4
Calcarine sulcus (posterior part)	0	−102	2	2.7*

*$p < .005$.

sponded in a different way (motor vs. verbal), this pattern was very similar to the one found by Mellet, Tzourio-Mazoyer et al. (2000). The replication of this pattern of activation in an independent sample provides strong evidence for the role of associative visual areas in this complex imagery task.

The behavioral results were also similar to those previously reported in the same mental imagery task (Mellet, Tzourio-Mazoyer et al., 2000). In addition, in the present study we report the horizontal eye movements recorded during the imagery task. The fact that the amplitude of eye movements was larger during imagery than in the baseline or rest conditions is in agreement with previous studies that reported such eye movements during the scanning of detailed mental images (Pollen & Trachtenberg, 1972). Mental scanning is reflected by the bilateral parieto-frontal network that was activated in the present study. Indeed, some researchers have suggested that this network plays a key role in spatial working memory and spatial mental imagery (Mellet, Bricogne et al., 2000). The ventral pathway, evident in the bilateral occipito-temporal activation, was also involved in our task. These areas have been found activated in previous studies of visual mental imagery (Ishai, Ungerleider, & Haxby, 2000; O'Craven & Kanwisher, 2000; Mellet, Tzourio, Denis, & Mazoyer, 1998; D'Esposito et al., 1997).

Deactivation and Activation in Medial Occipital Cortex During Both Mental Imagery Tasks (Figure 3)

The deactivations present in both imagery tasks were localized within the medial portion of the calcarine cortex. This result, together with similar deactivations previously reported, strongly shows that this early visual area is not necessary for all types of mental imagery tasks (Mellet, Tzourio-Mazoyer et al., 2000; Buckner, Raichle, Miezin, & Petersen, 1996). Moreover, a significant decrease in activity argues against the possibility that a lack of sensitivity could explain the failure to detect activation within this visual area. This relative rCBF decrease was present in the imagery task during both the silent and noise conditions, and thus is likely to be related to the nature of the imagery task. Indeed, Thompson and Kosslyn (2000) proposed that, unlike object imagery, spatial imagery does not rely on early visual cortex. The imagery task used here included a strong spatial component (the subjects needed to arrange the shapes properly, and judge relative heights). Interestingly, the part of the calcarine cortex and nearby cortex that we found deactivated here have been found to be activated in some other mental imagery studies (restricted to imagery with the eyes closed, Klein, Paradis, Poline, Kosslyn, & Le Bihan, 2000; Bookheimer et al., 1998; Kosslyn, Thompson, Kim, & Alpert, 1995; Kosslyn et al., 1996, 1999). The fact that most of these studies dealt with object imagery is consistent with the hypothesis that the nature of the imagery task (i.e., object vs. spatial) could in part be responsible for the different findings reported by different laboratories.

In addition to this deactivation of the medial part of the calcarine cortex, we observed a trend for an increase in rCBF in the most posterior part of the

calcarine cortex when the imagery task was performed in the noisy environment. We detected this increase in the comparison between noise and silent conditions and in the direct comparison between the noise and the silent conditions of the imagery task. The interpretation of such activation remains unclear. One may suggest that it reflects an increase of the visual attentional load related to the disruption induced by the noise. In fact, early visual areas could be more active when visual attention is more sustained (Kanwisher & Wojciulik, 2000; Kastner & Ungerleider, 2000), even in absence of any visual stimulation (Kastner, Pinsk, De Weerd, Desimone, & Ungerleider, 1999). However, this suggestion must be tempered because these recent studies and reviews emphasized that the modulation of activity in V1 due to attention may be less important than in the other retinotopically organized areas, such as V3 and V4. Moreover, the absence of an effect of noise in the frontal and parietal areas, which have been proposed to originate the top-down modulation in retinotopically organized areas (Kanwisher & Wojciulik, 2000), is not consistent with the attentional explanation.

Furthermore, our results indicated that poorer performance was accompanied by greater blood flow within the calcarine cortex during the silent imagery condition. We might hypothesize that during the noisy condition, there was no link between blood flow values in the calcarine cortex and accuracy because of, essentially, a ceiling effect: This posterior portion of calcarine cortex was activated for all subjects when they performed the task in a noisy environment. This idea is in agreement with our finding generally greater calcarine cortex activation in this region during the imagery$_{No}$ condition as compared to the imagery condition. Moreover, our results indicated that there was no relationship between the blood flow values in the calcarine cortex and response times. And, the lack of a speed–accuracy tradeoff was evident in the nonsignificant correlation between response times and accuracy.

Finally, we interviewed the subjects about their strategies, and their responses were consistent with our inferences. In the silent environment, subjects claimed that they had no difficulty generating and maintaining the mental image, spending most of the time transforming the mental image in order to assess the difference in height between the two cued portions of the figures (most of the subjects reported that they had to ''zoom in on'' the top of the figures). The reverse pattern was observed in the noisy environment: The subjects now reported having more difficulty maintaining a vivid mental image. Indeed, most of them claimed that their images faded more quickly in the presence of noise than in silent environment. If we take such reports at face value, they suggest that calcarine cortex might play a role in maintaining static images: The more the subject has to work to maintain a clear and vivid image, the more activity is present in the calcarine cortex. We found both degraded performance and increased activation of calcarine cortex when subjects performed the task in the presence of noise. These findings are consistent with the idea that such activation arose because the subjects had to work harder to maintain the image in the presence of noise.

Effect of fMRI Noise on Nonvisual Areas

The dorsal anterior cingulate cortex was more activated in imagery during noise than during silence. This area may play a key role in evaluative processes required to solve complex tasks and to detect situations where errors are likely to occur (MacDonald et al., 2000; Carter et al., 1998). Such processes probably are more engaged in the presence of disrupting noise; the degraded performance observed in imagery during noise is consistent with the claim that the anterior cingulate cortex acts as an error checking system (Kiehl et al., 2000). Note that in most of studies dealing with selective attention, anterior cingulate activation has been interpreted as related to an interference effect between relevant and irrelevant information. In the present study, there is no interference per se between the noise and the imagery task, but rather there was a general disrupting effect of the gradient sound. The present anterior cingulate cortex activation could thus suggest that this area plays a general role in evaluative processes, being involved even when an irrelevant stimulus (here the noise) does not compete with the processing of the target (here the mental image).

We found an effect of noise in the left posterior temporal cortex corresponding to the Wernicke's area. This result is consistent with a previous report that ambient scanner noise could activate language areas because of its complex periodic properties (Ulmer, Biswal, Yetkin, et al., 1998). Alternatively, the increase of attention load required to process the verbally delivered statements may have enhanced the activity in this region (Woodruff et al., 1996).

fMRI Noise and Auditory Cortex

When compared to silent rest, the fMRI gradient sound activated both primary (i.e., Heschl's gyrus) and associative auditory areas, a result in agreement with those of previous studies (Shah, Jäncke, Grosse-Ruyken, & Muller-Gartner, 1999; Bandettini et al., 1998; Ulmer, Biswal, Mark, et al., 1998). Moreover, these activations were located in the posteromedial part of Heschl's gyrus, which has been shown to process high-frequency tones. A critical point is that the auditory cortex was not equally activated in the comparisons of noise versus silent conditions. In fact, although auditory cortex was more activated (bilaterally) in the imagery task during noise than during silence, we found no such activation

during the baseline task in the two conditions; this finding shows that auditory cortex was activated as strongly in the silent baseline condition as in the noise baseline condition. Researchers have shown that auditory attention enhances the activity in the auditory cortex (Jäncke et al., 1999; Tzourio et al., 1997), and it is possible that auditory attention during silent baseline enhanced auditory cortex activity, thereby masking the activation related to the noise.

Conclusions

These findings have several general implications for the design and interpretation of fMRI studies. First, we have shown that fMRI noise degrades performance in a demanding, purely mental task. The same is likely to occur with other complex mental tasks, such as mental calculation and reasoning. These findings do not preclude the use of fMRI for the study of such abilities, but must be taken into account when interpreting the results. In particular, performance recorded off-line (e.g., during pretesting or after training) may not directly reflect the processing that occurs when subjects are in an fMRI magnet. Second, fMRI noise also altered the pattern of neural activation. Noise did not have a purely additive effect on neural activation, but affected some areas—such as the anterior cingulate—more than others. This additional activation was not a consequence of the task itself but reflected the interaction between task execution and noise. In the framework of the so-called imagery debate, we paid particular attention to early visual areas. We observed increased activity in calcarine cortex when the imagery task was performed in the fMRI-like sound environment. However, this effect was greater when subjects performed more poorly and had to work harder to maintain the mental images in the presence of noise.

METHODS

Subjects

Six right-handed male French students (age 18–22) volunteered to participate in this study. All were free of nervous disease or injury and had no abnormality in their T1-weighted MRI. Written informed consent was obtained from each subject after the procedures had been fully explained. This study was approved by the local ethics committee. In order to ensure optimal homogeneity of the sample of the subjects with respect to their imagery abilities, subjects were selected as ''high imagers'' (or, more specifically, as having high spatial ability) on the basis of their scores on the Minnesota Paper Form Board (MPFB) and on the Mental Rotations Test (MRT); all subjects scored beyond the 75th percentile of a population of 208 male subjects. The mean MPFB score for the subjects was 24.5 ± 1.9 (mean ± *SD*) and their mean MRT score was 18 ± 1.9.

Materials

fMRI Noise Recording and Playback

The sound produced by a clinical EPI-BOLD sequence was recorded using a nonmagnetic microphone near the radio frequency head coil (GE sigma 1.5 T; TR = 6 sec; TE = 60 msec; FA = 90 sec). In order to obtain the profile and the spectrum of the fMRI sound noise, the microphone output was coupled to a PC via a 12-bit ADC plug-in card with 20-kHz sampling for digitization. The scanner noise signal was Fourier-transformed to visualize the frequency spectrum and the mean acoustic noise level was also quantified with a sound-level meter (98 dB). The microphone was also plugged to a digital audiotape (DAT) for recording.

During the PET experiment, the sound was played back from the DAT and delivered through loudspeakers in the PET room. The noise level was set and the frequency spectrum was equalized in order to match the actual sound from the fMRI. This procedure allowed us to ensure that the sound played back in the PET room was as close as possible to the sound produced during an fMRI scan. The profile and the spectrum of both the original and the reproduced fMRI noise are displayed in Figure 4. The subjects wore earplugs to simulate further the standard fMRI acquisition conditions (Cho et al., 1997).

Mental Imagery Task

This task was adapted from that used in a previous study (Mellet, Tzourio-Mazoyer et al., 2000). In the mental imagery task the subjects were asked to judge subtle aspects of prelearned 3-D geometric scenes. The 3-D scenes were constructed by randomly placing four shapes on a base: a red triangle, a green rectangle, a yellow cube, and a blue cone (Figure 1).

Training phase. Subjects first participated in a training phase, prior to scanning, in a silent environment. During this stage, they memorized two scenes, which were identified as ''1'' and ''2.'' Prior to learning the scenes proper, subjects first memorized the base, including the letters and their precise positions. They were then shown the geometric shapes, one at a time, and were asked to memorize their appearance. The subjects were requested to memorize a complete scene as accurately as possible. After studying a scene, the subjects closed their eyes and visualized it, and then opened their eyes and compared the image against the actual stimulus, correcting their mental image if necessary. This procedure was repeated until the subjects felt that their mental image corresponded to the display. The stimuli

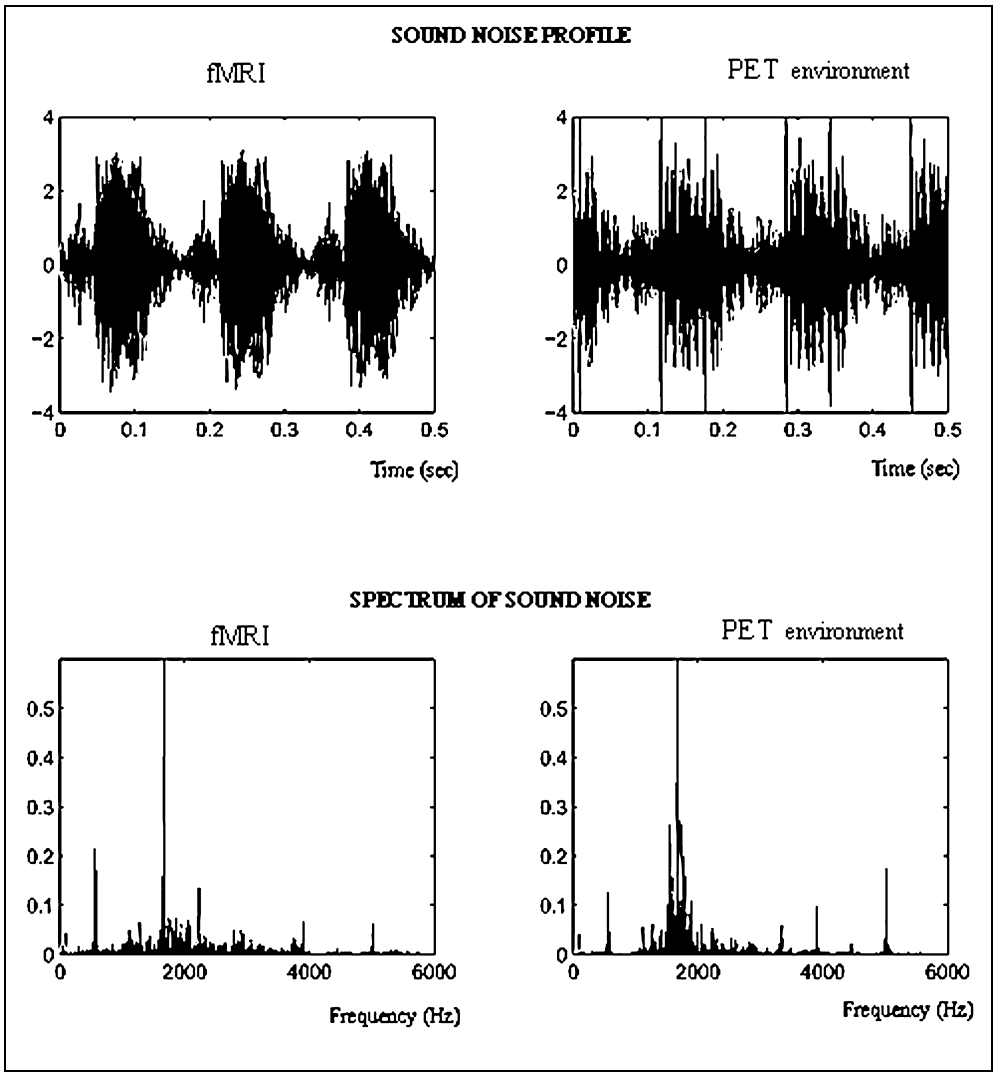

Figure 4. Profile and spectrum of the noise produced during fMRI (left) and of the sound played back in the PET room (right).

remained in free view until the subjects claimed that they had memorized the display. The same procedure was used with Scene "2."

After the subjects had memorized the initial two scenes, they were trained to perform the mental imagery task proper: With eyes closed, they first heard the identifying number of one of the two scenes through earphones, which prompted them to generate a mental image of the scene, as accurately as possible, with sharp corners and edges. Four seconds later, they heard a statement corresponding to a height comparison term, such as "D lower than B," which cued them to decide whether the heights of the shapes immediately above the named points were as described (i.e., in this case, the height of the figure at Point D was lower than that of the figure at Point B; see Figure 1, dotted lines). The subjects either pressed a "right" or "wrong" button, depending on their decision; if they were not able to respond, they pressed a third button. The subjects were asked to answer as quickly and accurately as possible (but with no time limit). Then, 750 msec after the subjects responded, the identification number of the other scene was delivered. The subjects then generated the corresponding mental image, and 4 sec later they heard a height comparison for Scene "2." The statements were delivered and the response and response time were recorded using Superlab software (Cedrus, Phoenix, AZ).

At the end of the training session, the subjects were interviewed to ensure that they understood the nature of the learning procedure and task, and any confusion was corrected and questions answered.

In order to eliminate any interference caused by dimmed PET room light, we enclosed the PET tomograph in a black tent-like chamber. We measured, with a light-level meter (TESTO 545, CORAME, Mont Saint-Aignan, France), the light intensity, which was 0 lx inside the chamber and 1 lx outside the chamber. In addition, all subjects had their eyes closed during PET acquisition.

Eye Movement Recording

In order to monitor spontaneous eye movements during the tasks, horizontal electrooculograms (EOG) were recorded for each subject using surface electrodes

placed at the outer canthi and at the right ear for a reference. Our EOG system can detect saccades greater than 1° of visual angle, and was calibrated before each condition. All EOG records were analyzed using dedicated software (SAMO) that detects saccadic components and quantifies the amplitude and frequency of spontaneous saccadic eye movements.

PET Conditions

We monitored rCBF in six different conditions, half in silence and half in noise. Those in silence we refer to as imagery, baseline, and rest; those in noise we will refer to as $\text{imagery}_{\text{No}}$, $\text{baseline}_{\text{No}}$, and rest_{No}. All conditions were replicated twice in five subjects and once in one subject.

For both imagery conditions, the subjects memorized two scenes during the 5 min prior to scanning. The scenes were memorized using the procedure described in the training session. During the PET measurements, the subjects performed the mental imagery task, with the cues and comparison statements delivered through earphones. A different set of nine comparison terms was used in each of the conditions in each replication, so that the subjects could not know in advance which statements they would have to assess.

During the baseline tasks, the subjects closed their eyes and listened to randomly chosen comparison statements delivered every 7 sec, and alternatively pressed the ''right'' and ''wrong'' button after each term. The subjects were instructed not to produce mental images. Although the subjects had at this point already gone through the training phase, and thus knew the nature of the task, they all reported, in the course of the posttest debriefing, that they could refrain from forming images or performing the task during the baseline measurements. We ensured that all the statements delivered through the earphones during the noisy version of the imagery and baseline tasks were clearly heard by the subjects.

The rest control conditions consisted in lying silently with eyes closed, as in all conditions, with no particular instruction except to refrain from moving. The brain areas engaged during rest have been studied elsewhere (Mazoyer et al., 2001).

Image Data Acquisition

For each rCBF measurement, 63 2.425-mm thick continuous brain slices were acquired simultaneously on an ECAT-HR+ PET camera (Siemens, Erlangen, Germany). Emission data were acquired in 3-D mode. Tasks were started 20 sec before the automated intravenous infusion of about 8 mCi of ^{15}O-labeled water. A single 90-sec scan was acquired and reconstructed (including a correction for head attenuation using a measured transmission scan) with a Hanning filter of 0.5 mm^{-1} cut off frequency and a pixel size of 2×2 mm^2. The between-scan time delay was 8 min, and the condition order was randomized in all subjects.

Data Analysis

After automatic realignment (using Automated Image Registration software; Woods, Grafton, Holmes, Cherry, & Mazziotta, 1997), the original brain images were transformed into the standard stereotactic Talairach space using the Montreal Neurological Institute (MNI) template. The images were smoothed using a Gaussian filter of 12-mm FWHM leading to a final smoothness of 15-mm FWHM. The rCBF was normalized within and between subject using a proportional model (scaling).

The comparisons across conditions were made by way of t statistics. Statistical parametric maps, corresponding to comparisons between the six conditions, were generated with the 1999 version of the SPM software (http://www.fil.ion.ucl.ac/spm/spm99.html). The experimental protocol was designed to use both rest and baseline conditions as control conditions for both imagery tasks. For each comparison (imagery vs. baseline and $\text{imagery}_{\text{No}}$ vs. $\text{baseline}_{\text{No}}$), the voxel amplitude t map was transformed in a Z volume that was thresholded at $Z = 3.09$, which correspond to a .001 confidence level (uncorrected for multiple comparisons).

A conjunction analysis using orthogonalized conditions was computed (Price & Friston, 1997) in order to reveal activations and deactivations common to both the imagery and $\text{imagery}_{\text{No}}$ conditions, when compared to baseline and $\text{baseline}_{\text{No}}$ conditions, respectively. The corresponding activation maps were thresholded at a .001 confidence level (uncorrected for multiple comparisons).

A comparison of $\text{imagery}_{\text{No}}$ versus $\text{baseline}_{\text{No}}$ and imagery versus baseline activation maps were computed in order to highlight activations that were specific or higher in the $\text{imagery}_{\text{No}}$ task as compared to the imagery task and thresholded at $p = .001$ (uncorrected for multiple comparisons). In order to avoid any artifactual activation in the contrast caused by a deactivation during imagery as compared to baseline, voxels that were not significant at $p = .05$ in the $\text{imagery}_{\text{No}}$ versus $\text{baseline}_{\text{No}}$ contrast were excluded.

In order to assess the effect of noise in each condition, the three conditions performed in the presence of noise (rest_{No}, $\text{baseline}_{\text{No}}$, and $\text{imagery}_{\text{No}}$) were compared with the three corresponding conditions performed in silence (rest, baseline, and imagery). For each comparison, the voxel amplitude t map was transformed in a Z volume that was thresholded at $p = .001$ confidence level (uncorrected for multiple comparisons).

In all cases, anatomical localization of the maximum Z score relied on an anatomical parcellation of the MNI template, which was based on the identification of the major sulci.

Acknowledgments

The authors are deeply indebted to their colleagues V. Beaudouin and G. Perchey for their invaluable help in tracer production and data acquisition. S.M. Kosslyn was supported by Grant 1 R01 MH60734-01 from the U.S. National Institutes of Health.

Reprint requests should be sent to Emmanuel Mellet, GIN, GIP Cyceron, BP 5229, 14074 Caen Cedex, France, or via e-mail: mellet@cyceron.fr.

REFERENCES

Bandettini, P. A., Jesmanowicz, A., Van Kylen, J., Birn, R. M., & Hyde, J. S. (1998). Functional MRI of brain activation induced by scanner acoustic noise. *Magnetic Resonance in Medicine, 39,* 410–416.

Bookheimer, S. Y., Zeffiro, T. A., Blaxton, T. A., Gaillard, W. D., Malow, B., & Theodore, W. H. (1998). Regional cerebral blood flow during auditory responsive naming: Evidence for cross-modality neural activation. *NeuroReport, 9,* 2409–2413.

Buckner, R. L., Raichle, M. E., Miezin, F. M., & Petersen, S. E. (1996). Functional anatomic studies of memory retrieval for auditory words and visual pictures. *Journal of Neuroscience, 16,* 6219–6235.

Carter, C. S., Braver, T. S., Barch, D. M., Botvinick, M. M., Noll, D., & Cohen, J. D. (1998). Anterior cingulate cortex, error detection, and the online monitoring of performance. *Science, 280,* 747–749.

Cho, Z.-H., Chung, S.-C., Lim, D.-W., & Wong, E. K. (1998). Effects of the acoustic noise of the gradient systems on fMRI: A study on auditory, motor and visual cortices. *Magnetic Resonance in Medicine, 39,* 331–335.

Cho, Z. H., Park, S. H., Kim, J. H., Chung, S. C., Chung, S. T., Chung, J. Y., Moon, C. W., Yi, J. H., Sin, C. H., & Wong, E. K. (1997). Analysis of acoustic noise in MRI. *Magnetic Resonance Imaging, 15,* 815–822.

Coull, J. T. (1998). Neural correlates of attention and arousal: Insights from electrophysiology, functional neuroimaging and psychopharmacology. *Progress in Neurobiology, 55,* 343–361.

D'Esposito, M., Detre, J. A., Aguirre, G. K., Stallcup, M., Alsop, D. C., Tippet, L. J., & Farah, M. J. (1997). A functional MRI study of mental image generation. *Neuropsychologia, 35,* 725–730.

Elliott, M. R., Bowtell, R. W., & Morris, P. G. (1999). The effect of scanner sound in visual, motor, and auditory functional MRI. *Magnetic Resonance in Medicine, 41,* 1230–1235.

Ishai, A., Ungerleider, L. G., & Haxby, J. V. (2000). Distributed neural systems for the generation of visual images. *Neuron, 28,* 979–990.

Jäncke, L., Buchanan, T., Lutz, K., Specht, K., Mirzazade, S., & Shah, N. J. S. (1999). The time course of the BOLD response in the human auditory cortex to acoustic stimuli of different duration. *Cognitive Brain Research, 8,* 117–124.

Kanwisher, N., & Wojciulik, E. (2000). Visual attention: Insights from brain imaging. *Nature Reviews, 1,* 91–100.

Kastner, S., Pinsk, M. A., De Weerd, P., Desimone, R., & Ungerleider, L. G. (1999). Increased activity in human visual cortex during directed attention in the absence of visual stimulation. *Neuron, 22,* 751–761.

Kastner, S., & Ungerleider, L. G. (2000). Mechanisms of visual attention in the human cortex. *Annual Review of Neuroscience, 23,* 315–341.

Kiehl, K. A., Liddle, P. F., & Hopfinger, J. B. (2000). Error processing and the rostral anterior cingulate: An event-related fMRI study. *Psychophysiology, 37,* 216–223.

Klein, I., Paradis, A.-L., Poline, J.-B., Kosslyn, S. M., & Le Bihan, D. (2000). Transient activity in the human calcarine cortex during visual–mental imagery: An event-related fMRI study. *Journal of Cognitive Neuroscience, 12,* 15–23.

Kosslyn, S. M., & Ochsner, K. N. (1994). In search of occipital activation during visual mental imagery. *Trends in Neurosciences, 17,* 290–292.

Kosslyn, S. M., Pascual-Leone, A., Felician, O., Camposano, S., Keenan, J. P., Thompson, W. L., Ganis, G., Sukel, K. E., & Alpert, N. M. (1999). The role of area 17 in visual imagery: Convergent evidence from PET and rTMS. *Science, 284,* 167–170.

Kosslyn, S. M., Shin, L. M., Thompson, W. L., McNally, R. J., Rauch, S. L., Pitman, R. K., & Alpert, N. M. (1996). Neural effects of visualizing and perceiving aversive stimuli: A PET investigation. *NeuroReport, 7,* 1569–1576.

Kosslyn, S. M., Thompson, W. L., & Alpert, N. M. (1997). Neural systems shared by visual imagery and visual perception: A positron emission tomography study. *Neuroimage, 6,* 320–334.

Kosslyn, S. M., Thompson, W. L., Kim, I. J., & Alpert, N. M. (1995). Topographical representations of mental images in primary visual cortex. *Nature, 378,* 496–498.

MacDonald, A. W., III, Cohen, J. D., Stenger, V. A., & Carter, C. S. (2000). Dissociating the role of the dorsolateral prefrontal and anterior cingulate cortex in cognitive control. *Science, 288,* 1835–1838.

Mazoyer, B., Zago, L., Mellet, E., Bricogne, S., Etard, O., Houde, O., Crivello, F., Joliot, M., Petit, L., & Tzourio-Mazoyer, N. (2001). Cortical networks for working memory and executive functions sustain the conscious resting state in man. *Brain Research Bulletin, 54,* 287–298.

Mellet, E., Bricogne, S., Tzourio-Mazoyer, N., Ghaëm, O., Petit, L., Zago, L., Etard, O., Berthoz, A., Mazoyer, B., & Denis, M. (2000). Neural correlates of topographical mental exploration: The impact of route versus survey perspective learning. *Neuroimage, 12,* 588–600.

Mellet, E., Petit, L., Mazoyer, B., Denis, M., & Tzourio, N. (1998). Reopening the mental imagery debate: Lessons from functional anatomy. *Neuroimage, 8,* 129–139.

Mellet, E., Tzourio, N., Denis, M., & Mazoyer, B. (1998). Cortical anatomy of mental imagery of concrete nouns based on their dictionary definition. *NeuroReport, 9,* 803–808.

Mellet, E., Tzourio-Mazoyer, N., Bricogne, S., Denis, M., Kosslyn, S. M., & Mazoyer, B. (2000). Functional anatomy of high-resolution visual mental imagery. *Journal of Cognitive Neuroscience, 12,* 98–109.

O'Craven, K. M., & Kanwisher, N. (2000). Mental imagery of faces and places activates corresponding stimulus-specific brain regions. *Journal of Cognitive Neuroscience, 12,* 1013–1023.

Pollen, D. A., & Trachtenberg, M. C. (1972). Alpha rhythm and eye movements in eidetic imagery. *Nature, 237,* 109 –112.

Price, C. J., & Friston, K. J. (1997). Cognitive conjunction: A new approach to brain activation experiments. *Neuroimage, 5,* 261–270.

Ravicz, M. E., Melcher, J. R., & Kiang, N. Y. (2000). Acoustic noise during functional magnetic resonance imaging. *Journal of the Acoustical Society of America, 108,* 1683–1696.

Roland, P. E., & Gulyãs, B. (1994). Visual imagery and visual representation. *Trends in Neurosciences, 17,* 1281 –287.

Shah, N. J., Jäncke, L., Grosse-Ruyken, M. L., & Muller-Gartner, H. W. (1999). Influence of acoustic masking noise in fMRI of the auditory cortex during phonetic discrimination. *Journal of Magnetic Resonance Imaging, 9,* 19–25.

Tagaris, G. A., Kim, S. G., Strupp, J. P., Andersen, P., Ugurbil, K., & Georgopoulos, A. P. (1997). Mental rotation studied by functional magnetic resonance imaging at high field (4 Tesla):

Performance and cortical activation. *Journal of Cognitive Neuroscience, 9,* 419–432.

Talavage, T. M., Edmister, W. B., Ledden, P. J., & Weisskoff, R. M. (1999). Quantitative assessment of auditory cortex responses induced by imager acoustic noise. *Human Brain Mapping, 7,* 79–88.

Talavage, T. M., Ledden, P. J., Benson, R. R., Rosen, B. R., & Melcher, J. R. (2000). Frequency-dependent responses exhibited by multiple regions in human auditory cortex. *Hearing Research, 150,* 225–244.

Thompson, W. L., & Kosslyn, S. M. (2000). Neural systems activated during visual mental imagery: A review and meta-analyses. In A. W. Toga & J. C. Maziotta (Eds.), *Brain mapping: II. The systems* (pp. 535–560). San Diego, CA: Academic Press.

Thompson, W. L., Kosslyn, S. M., Sukel, K. E., & Alpert, N. M. (2001). Mental imagery of high- and low-resolution gratings activates Area 17. *Neuroimage, 14,* 454–464.

Tzourio, N., Massioui, F. E., Crivello, F., Joliot, M., Renault, B., & Mazoyer, B. (1997). Functional anatomy of human auditory attention studied with PET. *Neuroimage, 5,* 63–77.

Ulmer, J. L., Biswal, B. B., Mark, L. P., Mathews, V. P., Prost, R. W., Millen, S. J., Garman, J. N., & Horzewski, D. (1998). Acoustic echoplanar scanner noise and pure tone hearing thresholds: The effects of sequence repetition times and acoustic noise rates. *Journal of Computer Assisted Tomography, 22,* 480–486.

Ulmer, J. L., Biswal, B. B., Yetkin, F. Z., Mark, L. P., Mathews, V. P., Prost, R. W., Estkowski, L. D., McAuliffe, T. L., Haughton, V. M., & Daniels, D. L. (1998). Cortical activation response to acoustic echo planar scanner noise. *Journal of Computer Assisted Tomography, 22,* 111–119.

Woodruff, P. W., Benson, R. R., Bandettini, P. A., Kwong, K. K., Howard, R. J., Talavage, T., Belliveau, J., & Rosen, B. R. (1996). Modulation of auditory and visual cortex by selective attention is modality-dependent. *NeuroReport, 7,* 1909–1913.

Woods, R. P., Grafton, S. T., Holmes, C. J., Cherry, S. R., & Mazziotta, J. C. (1997). Automated image registration: I. General methods and intrasubject validation. *Journal of Computer Assisted Tomography, 22,* 139–152.